# Diabetes-Induced Inhibition of Voltage-Dependent Calcium Channels in the Retinal Microvasculature: Role of Spermine

*Kenji Matsushita,*[1] *Masanori Fukumoto,*[1] *Takatoshi Kobayashi,*[1] *Masato Kobayashi,*[1] *Eisuke Ishizaki,*[1] *Masahiro Minami,*[1] *Kozo Katsumura,*[1] *Sophie D. Liao,*[1] *David M. Wu,*[1] *Ting Zhang,*[1,2] *and Donald G. Puro*[1,3]

**Purpose.** Although decentralized control of blood flow is particularly important in the retina, knowledge of the functional organization of the retinal microvasculature is limited. Here, the authors characterized the distribution and regulation of L-type voltage-dependent calcium channels (VDCCs) within the most decentralized operational complex of the retinal vasculature—the feeder vessel/capillary unit—which consists of a capillary network plus the vessel linking it with a myocyte-encircled arteriole.

**Methods.** Perforated-patch recordings, calcium-imaging, and time-lapse photography were used to assess VDCC-dependent changes in ionic currents, intracellular calcium, abluminal cell contractility, and lumen diameter, in microvascular complexes freshly isolated from the rat retina.

**Results.** Topographical heterogeneity was found in the distribution of functional VDCCs; VDCC activity was markedly greater in feeder vessels than in capillaries. Experiments showed that this topographical distribution occurs, in large part, because of the inhibition of capillary VDCCs by a mechanism dependent on the endogenous polyamine spermine. An operational consequence of functional VDCCs predominantly located in the feeder vessels is that voltage-driven vasomotor responses are generated chiefly in this portion of the feeder vessel/capillary unit. However, early in the course of diabetes, this ability to generate voltage-driven vasomotor responses becomes profoundly impaired because of the inhibition of feeder vessel VDCCs by a spermine-dependent mechanism.

**Conclusions.** The regulation of VDCCs by endogenous spermine not only plays a critical role in establishing the physiological organization of the feeder vessel/capillary unit, but also may contribute to dysfunction of this decentralized operational unit in the diabetic retina. (*Invest Ophthalmol Vis Sci.* 2010;51:5979–5990) DOI:10.1167/iovs.10-5377

From the [1]Department of Ophthalmology and Visual Sciences and the [2]Eye and ENT Hospital, Fudan University, Shanghai, China; and the [3]Department of Molecular and Integrative Physiology, University of Michigan, Ann Arbor, Michigan.

Supported by National Eye Institute Grants EY12505 and EY07003, Research to Prevent Blindness, Inc., and a Heed Fellowship.

Submitted for publication February 12, 2010; revised April 6, 2010; accepted May 8, 2010.

Disclosure: **K. Matsushita**, None; **M. Fukumoto**, None; **T. Kobayashi**, None; **M. Kobayashi**, None; **E. Ishizaki**, None; **M. Minami**, None; **K. Katsumura**, None; **S.D. Liao**, None; **D.M. Wu**, None; **T. Zhang**, None; **D.G. Puro**, None

Corresponding author: Donald G. Puro, Department of Ophthalmology and Visual Sciences, University of Michigan, 1000 Wall Street, Ann Arbor, MI 48505; dgpuro@umich.edu.

In most mammals and all primates, visual function is dependent on an intraretinal vascular system that is highly adapted to the unique challenge of supplying oxygen and nutrients to a tissue whose translucency is essential for function. Consistent with the requirement that blood vessels minimally interfere with light, the retina has a relatively low density of capillaries.[1] However, this paucity of microvessels leaves little functional reserve for the vital task of matching local perfusion to metabolic demand. Thus, efficient coupling of blood flow to meet local needs is particularly important in the retina. As a likely adaptation to increase the efficient control of local perfusion, the circulatory system of the retina appears to be especially well developed for the decentralized regulation of blood flow. Indicative of this, the capillaries of the retina have the highest density of abluminal pericytes,[2] whose contractions and relaxations regulate lumen diameter and, thereby, capillary perfusion.[3,4]

Although decentralization is an important operational feature of the retina's circulatory system, much remains to be learned about how its microvasculature is functionally organized. To address this gap in knowledge, we characterized the distribution and regulation of functional L-type voltage-dependent calcium channels (VDCCs) within the feeder vessel/capillary unit of the normal and diabetic retina. This distal portion of the retinal microvasculature was of particular interest because evidence is accumulating that a capillary network plus the feeder vessel linking it with a myocyte-encircled arteriole constitute a functional unit in which cell-to-cell transmission by way of gap junctions is highly efficient.[5,6,7] We focused on VDCCs because though they are known to be critically important in the generation of voltage-driven vasomotor responses in arteries and arterioles, the location and regulation of these ion channels within the retinal microvasculature are not well characterized. In this study, we also assessed the effect of diabetes on VDCC function because dysfunction of these channels may contribute to blood flow dysregulation and sight-threatening complications in the diabetic retina.

To facilitate the assessment of VDCC-dependent changes in ionic currents, intracellular calcium, abluminal cell contractility, and lumen diameter in the feeder vessel/capillary unit, we studied microvascular complexes that were freshly isolated from the adult rat retina and included an arteriole whose outer diameter measured 12 to 18 $\mu$m, a precapillary feeder vessel with an outer diameter of 7 to 10 $\mu$m, and a network of capillaries with outer diameters of $<6$ $\mu$m. An experimental advantage of this preparation is that the abluminal cells of the capillaries, i.e., the pericytes, can easily be identified by the distinctive "bump on a log" appearance of their somas, which are at a density of $\leq 4$ somas/100 $\mu$m.[8] Also easily identified are the closely packed ($\geq 5$ somas/100 $\mu$m) dome-shaped ablumi-

nal (mural) cells of the feeder vessels.[5,8] Thus, it was fairly straightforward to use the patch-clamp technique, calcium-imaging, and time-lapse photography to study the feeder vessel/capillary unit within freshly isolated retinal microvascular complexes.

This study revealed that there is a topographical heterogeneity in the distribution of functional L-type VDCCs. Namely, VDCC function is greater in the feeder vessels than in the capillaries. Our experiments indicated that endogenous spermine, a polyamine known to inhibit L-type calcium channels,[9–13] plays an important role in establishing the topographical distribution of functional VDCCs within the feeder vessel/capillary unit. We also report that early in the course of streptozotocin-induced diabetes, a boost in the spermine-mediated inhibition of VDCCs markedly diminishes voltage-driven vasomotor responses in the feeder vessel/capillary unit. Thus, our findings support the idea that spermine has a pathophysiological, as well as a physiological, role in the regulation of VDCC function in the microvasculature of the retina.

## METHODS

Animal use conformed to the guidelines of the ARVO Statement for the Use of Animals in Ophthalmic and Vision Research and was approved by the University of Michigan Committee on the Use and Care of Animals. This study used 129 Long-Evans rats (Charles River, Cambridge, MA) given food and water ad libitum and maintained on a 12-hour light/12-hour dark cycle.

### Model of Diabetes

Diabetes was induced by one or two intraperitoneal injections of streptozotocin (150 mg/kg diluted in 0.8 mL citrate buffer) into 5- or 6-week-old Long-Evans rats that had fasted for 5 hours. This study used 24 rats made hyperglycemic for 6.8 ± 0.5 weeks. At the time of kill, the diabetic rats were 11.7 ± 0.7 weeks old, which was not a significantly different age from that of the nondiabetic rats used in this study (10.1 ± 0.4) weeks. Immediately before microvessels were harvested from diabetic rats, the blood glucose level was 318 ± 14 mg/dL; the blood glucose level in the nondiabetic rats was 90 ± 2 mg/dL.

### Microvessel Isolation

Using a tissue print procedure described previously,[5,8] microvascular complexes were isolated from the retinas of adult rats that were killed with rising concentrations of carbon dioxide. In brief, retinas were rapidly removed and, after the removal of adherent vitreous, were incubated for approximately 24 minutes at 30°C in Earle's balanced salt solution supplemented with 0.5 mM EDTA, 6 U papain (Worthington Biochemicals, Freehold, NJ), and 2 mM cysteine. Subsequently, the retinas were cut into quadrants, each of which was gently compressed for approximately 30 seconds between glass coverslips (Warner Instrument Corp., Hamden, CT); microvessels adhered to the coverslip touching the retina's vitreal surface. A schematic drawing of the portion of the retinal vasculature isolated by this technique is shown in Figure 1. Unless otherwise noted, each microvascular complex used in this study included an arteriole encircled by "doughnut-shaped" myocytes, a precapillary feeder vessel whose abluminal (mural) cells have "dome-shaped" somas at a density of ≥5/100 μm and a capillary network whose abluminal cells (pericytes) appear as "bumps on a log" and have a density of ≤4/100 μm. Illustrations of freshly isolated retinal microvascular complexes are available.[5,8] In some experiments, the capillary network was separated from the proximal microvasculature, as detailed previously.[5] Unless otherwise noted, microvessels were used within 5 hours after isolation; experiments were performed at room temperature.

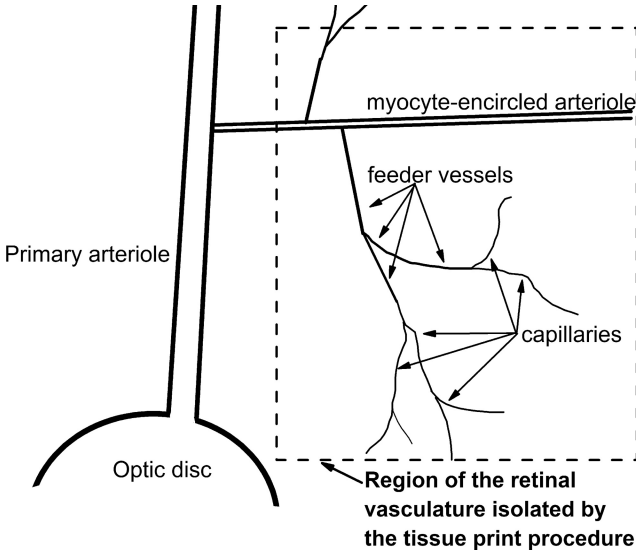


**FIGURE 1.** Schematic drawing in which the *dotted lines* enclose the portion of the rat retinal vasculature isolated by the tissue print procedure used in this study.

### Perforated-Patch Recordings

The bathing and pipette solutions used in our electrophysiological studies were designed to optimize the currents passing through VDCCs and to minimize $K^+$ conductances. In brief, a microvessel-containing coverslip was positioned in a recording chamber perfused with a solution containing 95 mM NaCl, 0.8 mM $MgCl_2$, 20 mM $BaCl_2$, 3 mM CsCl, 20 mM tetraethylammonium chloride, 5 mM glucose, and 10 mM HEPES at pH 7.4, with the osmolarity adjusted to approximately 310 mOsm/L. Recording micropipettes were filled with a solution consisting of 135 mM CsCl, 6 mM $MgCl_2$, 10 mM HEPES, 60 μg/mL amphotericin B, and 60 μg/mL nystatin at pH 7.4, with the osmolarity adjusted to approximately 280 mOsm/L. These micropipettes, which had resistances of 5 to 10 MΩ, were mounted in the holder of a patch-clamp amplifier (Axopatch 200B; MDS Analytical Technologies, Union City, CA) and positioned onto to an abluminal microvascular cell as described previously,[5,6,8] and then a ≥10 GΩ seal was established. Access resistances were <25 MΩ. Currents were filtered with a four-pole Bessel filter, digitally sampled and stored on a computer equipped with commercial software (pClamp, version 8.2 or 10; MDS Analytical Technologies, and Origin, version 7; OriginLab, Northampton, MA). A sketch or photomicrograph documented the location of the recording site. The calculated liquid junction potential was corrected for subsequent data collection.

We found that under the recording conditions used in this study, the detected currents were generated at sites relatively close to the recording pipette. Specifically, as shown in Figure 2, voltage decayed by approximately 95% over a microvascular length of 400 μm. Based on our previous documentation that the length of a precapillary feeder vessel is 422 ± 26 μm,[8] it appears that nearly all the current recorded at a site in the proximal portion of a feeder vessel was generated within the feeder vessel; conversely, recordings >400 μm distal to the feeder vessel/capillary junction detected currents generated predominantly in the capillaries. In addition, indicative of a relatively small portion of a microvessel held under a voltage-clamp, the membrane capacitances calculated according to the method of Zhao and Santos-Sacchi[14] were relatively small: 38 ± 9 pF ($n$ = 7) and 39 ± 8 pF ($n$ = 9) in nondiabetic feeder vessels and capillaries, respectively, and, 43 ± 20 pF ($n$ = 6) and 43 ± 14 pF ($n$ = 4) in diabetic feeder vessels and capillaries, respectively.

For most recordings, the pCLAMP-controlled voltage-clamp protocols consisted of voltage steps from holding potentials of −85 mV and −5 mV, voltages at which VDCC inactivation is minimal and maximal,

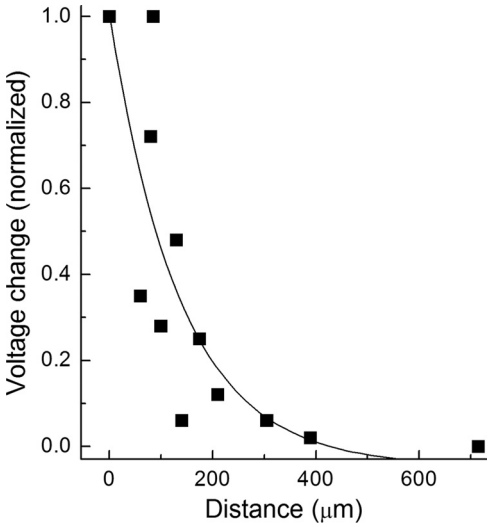


**FIGURE 2.** Voltage spread within retinal microvessels monitored under recording conditions used in this study. Solution B was miniperfused systematically at sites along a microvessel as voltage was monitored by a perforated-patch pipette. The amplitude of the hyperpolarization generated by the miniperfusion of solution B at the recording site was used to normalize the voltage changes detected when solution B was applied elsewhere. The *line* shows the fit for a first-order exponential decay. Three microvessels were assessed.

respectively.[15] The current-voltage relations of the VDCC current were calculated by subtracting the currents generated from the holding potential of −5 mV from those generated from the holding potential of −85 mV. In recordings designed to assess the effect nifedipine, which is a dihydropyridine whose block of L-type VDCCs is voltage dependent and is thereby diminished at hyperpolarized potentials,[16] voltage steps were generated from −55 mV and −5 mV. Current densities were calculated using the membrane capacitances listed.

## Calcium Imaging

As detailed previously,[17] freshly isolated retinal microvascular complexes were loaded with 5 μM fura-2AM (Molecular Probes, Eugene, OR) at 37°C for 30 minutes. After allowing the AM ester to be cleaved, a coverslip containing fura-loaded microvessels was positioned in a 200-μL recording chamber that was perfused (~1.5 mL/min) continuously. Digital imaging was performed with a microscope (Eclipse E600 FN; Nikon, Tokyo, Japan), an optical sensor (Sensicam; Cooke Corp., Auburn Hills, MI), and a high-intensity mercury lamp coupled to an monochromator (Optoscan; Cairn Research Ltd., Faversham, UK); imaging equipment and data collection were controlled with bioanalytical software (MetaFluor; Molecular Devices, Sunnyvale, CA). Fluorescence intensities were measured every 10 seconds at 340 nm and 380 nm within regions of interests (ROI), each of which encircled a single abluminal cell soma. Of note, isolated microvascular complexes lacked detectable autofluorescence. In addition, minimal fluorescence was derived from fura-2 that was insensitive to free $Ca^{2+}$ because of its being sequestered within cellular compartments or not fully de-esterified; exposure of fura-loaded microvessels to solution A supplemented with 2 mM $MnCl_2$ plus 5 μM ionomycin quenched 98.2% ± 0.1% ($n$ = 40) of the $F_{340}$ and 98.6% ± 0.1% ($n$ = 40) of the $F_{380}$. Given the minimal amount of fluorescence from fura-2 that was insensitive to free $Ca^{2+}$, $Mn^{2+}$ quenching was not routinely performed. Background fluorescence of the optical system was measured in each experiment by placing some ROIs in cell-free areas of the coverslip. After subtracting this background, the $F_{340}/F_{380}$ ratio was calculated and converted to the intracellular calcium concentration by use of the equation of Grynkiewicz et al.,[18] in which $R_{min}$ and $R_{max}$ were determined as detailed previously.[17]

In some experiments, microvessels were exposed to solutions (Table 1) that contained different concentrations of $K^+$ but whose concentration of other cations, osmolarity, and pH were identical. For certain experiments, microvessels were exposed to solution A supplemented with 5 mM spermine for 10 to 15 minutes before the onset of fluorescence measurements; 5 mM spermine was also in the perfusate during calcium imaging. In some of the experiments, microvessels were initially exposed for 20 to 23 hours in solution A supplemented with 5 mM difluoromethylornithine (DFMO). Because the $K^+$-induced calcium increases in pericytes located on nondiabetic and diabetic microvessels maintained in solution A for 1 to 5 hours and 20 to 23 hours after isolation from the retina were not significantly different ($P \geq 0.4$), values from these time periods were combined for the assays conducted with no additives. To determine the nifedipine sensitivity of the induced changes in cell calcium, microvessels were pre-exposed to solution A supplemented with 10 μM nifedipine for 10 to 15 minutes before fluorescence was monitored; of note, for these experiments, 10 μM nifedipine was present throughout the experiment. For each ROI, the baseline calcium concentration was the mean value during the 100 seconds immediately preceding exposure to solution D, solution C, or solution A supplemented with spermine. A VDCC-mediated increase in intracellular calcium was defined as the difference between the maximum change in abluminal cell calcium induced in the absence and in the presence of 10 μM nifedipine.

## Time-Lapse Photography

Contractile responses of abluminal cells and induced changes in the diameters of feeder vessels and capillaries were assessed with the aid of time-lapse photography, as detailed previously.[17,19–21] In brief, a microvessel-containing coverslip was positioned in a perfusion chamber (volume, 200 μL) on the stage of a camera (Eclipse E800; Nikon) equipped with differential interference contrast optics that permitted 1000× magnification with the aid of a 100× oil objective as images were recorded at 8-second intervals using a digital camera (DCM1200; Nikon) and image analysis software (ImagePro Plus, version 4.5; Media Cybernetics, Silver Spring, MD). Microvessels were monitored before, during, and after exposure to various solutions in the absence or presence of 10 μM nifedipine. For each monitored microvessel, the maximum induced narrowing of the lumen diameter was determined. Some microvessels were pre-exposed to solution A supplemented with 300 μM GAP 27 for 2 hours, a time period that eliminates gap junction transmission in retinal microvessels.[17] In some experiments, microvessels were incubated in solution A supplemented with 5 mM spermine for 10 to 20 minutes before assay. In other experiments, microvessels

**TABLE 1.** Composition of Various Solutions Used in This Study

| Solution | KCl | NaCl | NMDG-Cl | $CaCl_2$ | $MgCl_2$ | Na-Hepes | Mannitol | Glucose |
|---|---|---|---|---|---|---|---|---|
| A | 3 | 140 | — | 1.8 | 0.8 | 10 | 15 | 5 |
| B | 3 | 43 | 94.5 | 1.8 | 0.8 | 10 | 15 | 5 |
| C | 10 | 43 | 87.5 | 1.8 | 0.8 | 10 | 15 | 5 |
| D | 97.5 | 43 | — | 1.8 | 0.8 | 10 | 15 | 5 |

Values are given in mM.

were incubated in solution A supplemented with 5 mM DFMO for 20 to 23 hours before assay. Because the 97.5 mM $K^+$-induced contraction of feeder vessel mural cells that had been maintained in solution A for 1 to 5 hours or 20 to 23 hours were not significantly different ($P = 0.6$), values from these time periods were combined for the assays conducted with no additives. As shown previously,[17,19–21] determination of whether an abluminal cell contracted, relaxed, or remained unchanged during exposure to an experimental solution was made by careful visual inspection of the time-lapse movie. With the aid of image analysis software (ImagePro Plus, version 4.5; Media Cybernetics), changes in lumen diameters at sites adjacent to a contracting abluminal cell were quantified.

## Immunocytochemistry

This protocol was performed at room temperature, unless noted otherwise. After freshly isolated microvessels were fixed for 30 minutes with 4% paraformaldehyde in phosphate-buffered saline (PBS), endogenous peroxidase activity was blocked by 0.3% hydrogen peroxide for 30 minutes, and cell membranes were permeabilized by a 30-minute exposure to 0.5% Triton X-100. Microvessel-containing coverslips were then exposed for 16 hours at 4°C to a well-characterized[22] commercially available (Calbiochem, San Diego, CA) antibody (1:100) developed in rabbit using a synthetic peptide, TTKINMDDLQPSENEDKS, which corresponds to amino acids 818 to 835 of the $\alpha_{1C}$ calcium channel subunit of the rat brain. Omission of the primary antibody served as one of the controls; as another control, the primary antibody was preincubated with the synthetic peptide (Calbiochem) for 1 hour before application onto a microvessel-containing coverslip. After incubation with biotin-conjugated goat anti–rabbit IgG (Vector Laboratories, Burlingame, CA) at 1:200 for 1 hour, coverslips were kept in a horseradish peroxidase-streptavidin solution (RTU; Vector Laboratories) for approximately 40 hours at 4°C and then were exposed to the avidin-biotin-peroxidase complex (ABC method; Vector Laboratories) at 1:100 for 30 minutes. After development with diaminobenzidine, microvessels were examined with bright-field optics.

## Chemicals

Unless otherwise noted, chemicals were obtained from Sigma.

## Statistical Analysis

For the data given as mean ± SEM, probability was evaluated by the two-tailed Student's *t*-test. Data quantifying the contractile responses of abluminal cells were given as the percentage of all monitored abluminal cells that relaxed or contracted; statistical differences were evaluated using the Fisher exact test. $P \geq 0.05$ indicated lack of significant difference.

# Results

## Location of Functional Voltage-Dependent Calcium Channels

Perforated-patch recordings revealed that the density of the VDCC current was 7.5-fold larger ($P = 0.0015$) in the feeder vessels than in the capillaries of the retinal microvasculature (Fig. 3). This reflects a substantial difference in VDCC conductances because the membrane capacitances at feeder vessels and capillary sites were not significantly different (see Methods). Our electrophysiolog-

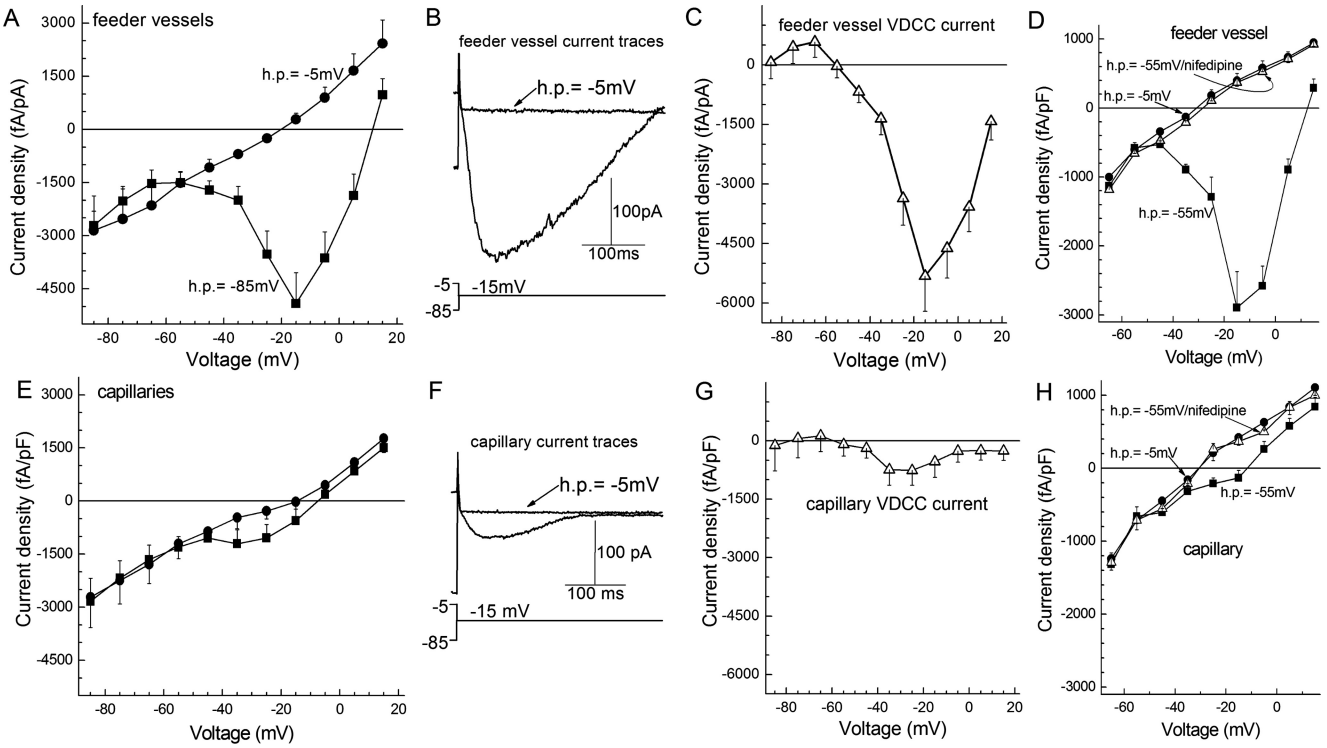


**Figure 3.** VDCC currents in feeder vessels and capillaries of the retinal microvasculature. (**A**) Plots of the peak inward current density versus test potential recorded from abluminal (mural) cells located on the primary branch of feeder vessels ($n = 7$). Currents were generated from holding potentials of −85 mV (*squares*) and −5 mV (*circles*). (**B**) Current traces recorded from a feeder vessel mural cell during voltage steps to −15 mV from holding potentials of −85 mV and −5 mV. (**C**) Difference of the plots in **A**. (**D**) Effect of nifedipine on the relationship between the peak inward current density in feeder vessels ($n = 4$) and the test potential in experiments using holding potentials of −5 mV (*circles*) and from −55 mV. *Squares*: no nifedipine. *Triangles*: 10 μM nifedipine. (**E**) Plots of the peak inward current density versus test potential recorded from the abluminal cells (pericytes) of capillaries ($n = 9$). Currents were generated from holding potentials of −85 mV (*squares*) and −5 mV (*circles*). (**F**) Current traces evoked by a voltage step from a holding potential of −85 mV or −5 mV. (**G**) Difference of the curves in (**E**). (**H**) Plots of the peak inward current density versus test potential recorded from capillary pericytes ($n = 3$). *Squares*: No nifedipine. *Triangles*: 10 μM nifedipine.

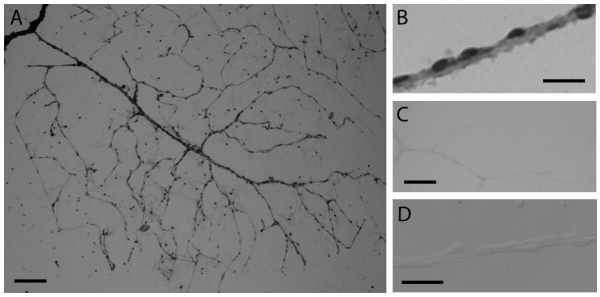


**FIGURE 4.** Immunoreactivity for the $\alpha_{1C}$ subunit of the L-type calcium channel. (**A**) Photomicrograph showing a microvascular complex freshly isolated from the rat retina and stained with an anti-$\alpha_{1C}$ subunit antibody. (**B**) Immunopositive abluminal cells on a retinal microvessel. (**C**) A microvascular complex that was prepared for immunocytochemistry in the absence of the primary antibody; staining of the feeder vessel/capillary complex was minimal. (**D**) A control in which the primary antibody was preincubated with the antigenic peptide before exposure of a microvascular complex to the antibody/antigenic peptide-containing solution; staining of the microvascular complex was minimal. Scale bars: (**A**, **C**) 100 $\mu$m; (**B**, **D**) 25 $\mu$m.

ical experiments also documented that the VDCC currents detected in feeder vessels and capillaries were near totally blocked by 10 $\mu$M nifedipine, a blocker of L-type VDCCs. Confirmation of the ability of nifedipine to block microvascular VDCC channels proved useful in subsequent studies in which calcium imaging and time-lapse photography were used to assess VDCC function.

From the data summarized in Figure 3, we concluded that most functional VDCCs in the feeder vessel/capillary unit were located in the feeder vessel portion. On the other hand, these results also suggested that some VDCC current is generated in the capillaries, though these experiments did not exclude the possibility that the VDCC current detected in the capillary network might have been generated in the feeder vessels and then transmitted distally. However, consistent with at least one class of L-type VDCCs expressed in retinal capillaries, we detected immunoreactivity for the $\alpha_{1C}$ calcium channel subunit at sites throughout the retinal microvasculature, including the capillaries (Fig. 4). Of note, it is unknown whether other $\alpha$ subunits of L-type VDCCs, such as $\alpha_{1D}$ and $\alpha_{1F}$, are also expressed in the retinal microvasculature. Additional evidence strongly supporting the concept that some VDCC current is, in fact, generated in the capillaries was obtained from perforated-patch recordings from capillaries that were physically separated from their feeder vessels. In isolated capillaries, we found that the density of the inward VDCC current was 820 ± 385 fA/pF ($n = 4$), which was not significantly different from the current density (590 ± 245 fA/pF; $n = 9$) recorded from capillaries that remained attached to the proximal microvasculature (Fig. 3G). Based on the experiments illustrated in Figures 3 and 4, we concluded that both feeder vessels and capillaries have VDCCs but that VDCC function occurs predominantly in the feeder vessels.

To complement our electrophysiological analyses of VDCC function, we monitored VDCC-dependent changes in the intracellular calcium concentration of cells located on the abluminal wall of feeder vessels and capillaries. An advantage of this experimental approach was that while our perforated-patch recordings detected VDCC currents generated from a population of microvascular cells, calcium imaging permitted the monitoring of VDCC-dependent changes in the calcium concentration of individual abluminal cells. In one series of calcium-imaging experiments designed to help determine the effect of VDCCs on the basal level of abluminal cell calcium, we caused the membrane potential of retinal microvessels to increase; this was useful because hyperpolarization causes inactivation of microvascular VDCCs.[15] We induced hyperpolarization by increasing the $K^+$ concentration of the perfusate from 3 mM (solution B) to 10 mM (solution C). As detailed in a previous study of the retinal microvasculature,[8] this 7-mM increase in extracellular $K^+$ resulted in a 14-mV hyperpolarization that was chiefly caused by enhanced $K^+$ efflux through inwardly rectifying $K^+$ channels. A similar physiologically relevant rise in $K^+$ is well known to cause hyperpolarization at numerous sites throughout the circulatory system.[23–25] In this study, we observed that switching from solution B (3 mM $K^+$) to solution C (10 mM $K^+$) resulted in a significant ($P < 0.0001$) decrease in the intracellular calcium concentration of mural cells located on feeder vessels (Fig. 5A). Consistent with this hyperpolarization-induced decrease in calcium being attributed to a decrease in the basal activity of VDCCs, this effect was profoundly blocked by nifedipine, which, as shown in Figure 3D, potently inhibits VDCC function in feeder vessels. Of note, although nifedipine can block voltage-insensitive, store-operated calcium channels in choroidal arteriolar smooth muscle,[26] inhibition of the store-operated channels is unlikely to account for the inhibition by this dihydropyr-

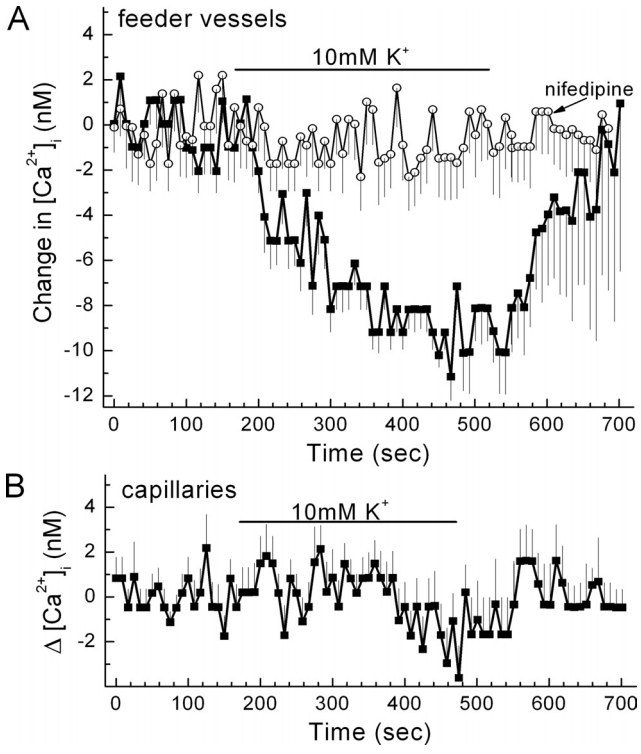


**FIGURE 5.** Effect of a 10 mM $K^+$-induced hyperpolarization on the intracellular calcium concentration of abluminal cells of feeder vessels and capillaries. (**A**) Plot of the mean change in intracellular calcium versus time for abluminal cells located on feeder vessels. Retinal microvessels were exposed to perfusates without (*squares*) or with (*circles*) 10 $\mu$M nifedipine. Initially, the perfusate was solution B (3 mM $K^+$) plus or minus nifedipine. Solutions B and C had identical osmolarities and identical $Na^+$ and $Cl^-$ concentrations. The *bar* shows when the perfusate was solution C (10 mM $K^+$) plus or minus nifedipine. The number of monitored cells was 16 and 13 for the nifedipine-free and the nifedipine-containing groups, respectively. The decrease in calcium during exposure to solution C was significant ($P < 0.0001$), as was the inhibitory effect of nifedipine ($P < 0.0001$). (**B**) Plot of the mean change in intracellular calcium versus time for capillary pericytes ($n = 19$). Initially, the perfusate was solution B (3 mM $K^+$); the *bar* shows when the perfusate was solution C (10 mM $K^+$).

idine of the voltage-induced changes in abluminal cell calcium. In contrast to the effect of the 10 mM $K^+$-induced hyperpolarization on mural cell calcium in the feeder vessels, the calcium concentration of capillary pericytes was not significantly affected (Fig. 5B). Thus, the experiments summarized in Figure 5 provide further support for the concept that VDCC function is greater in the mural cells of the feeder vessels than in the pericytes of the capillaries.

In other calcium-imaging experiments, we assessed the effect on abluminal cell calcium of depolarization, which activates microvascular VDCCs.[15] In these experiments, depolarization was induced by exposing retinal microvessels to a perfusate containing 97.5 mM $K^+$ (solution D), which causes a profound decrease in the membrane potential.[8] As illustrated in Figure 6A, exposure to the 97.5 mM $K^+$ solution resulted in a substantial increase in the concentration of calcium in the mural cells of the feeder vessels. Consistent with this depolarization-induced increase in mural cell calcium being caused by the activation of VDCCs, nifedipine eliminated this effect (Fig. 6A). Consistent with VDCC function being greater in feeder vessel mural cells than in capillary pericytes, the 97.5 mM $K^+$-induced depolarization resulted in only a modest rise in pericyte calcium (Fig. 6B). As summarized in Figure 7, the nifedipine-sensitive increase in abluminal cell calcium during exposure to 97.5 mM $K^+$ was significantly ($P < 0.0001$) greater in feeder vessels than in capillaries.

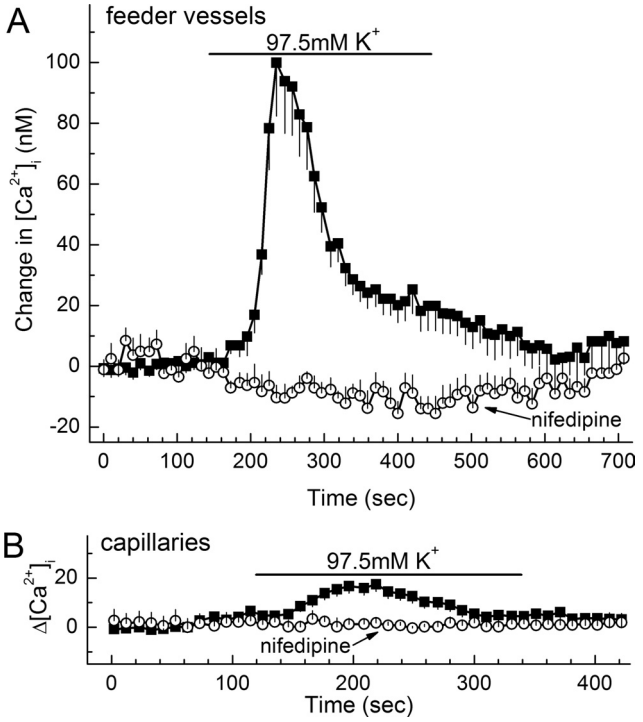


**FIGURE 6.** Effect of 97.5 mM $K^+$ on abluminal cell calcium in feeder vessels and capillaries. (**A**) Plot of the mean change in intracellular calcium versus time for abluminal cells located on feeder vessels. Initially, the perfusate was solution B (3 mM $K^+$) without or with 10 $\mu$M nifedipine. The *bar* shows when the perfusate was solution D (97.5 mM $K^+$ ± nifedipine). Solutions B and D had identical osmolarities and identical $Na^+$ and $Cl^-$ concentrations. The number of feeder vessel mural cells was 16 for both the nifedipine-free and the nifedipine-containing groups. The rise in calcium was significant ($P < 0.0001$) in the absence of nifedipine and was significantly ($P < 0.0001$) lower in the presence of this L-type VDCC blocker. (**B**) Plot of the mean change in pericyte calcium versus time during exposure to the same perfusates as used in (**A**). The number of monitored capillary pericytes was 43 and 12 for the nifedipine-free and the nifedipine-containing groups, respectively. The rise in pericyte calcium in the absence of nifedipine was significant ($P = 0.0002$); nifedipine significantly ($P = 0.0003$) blocked the depolarization-induced increase in intracellular calcium.

Based on the calcium-imaging studies summarized in Figures 5 to 7, we concluded that VDCC function in an abluminal cell located on a feeder vessel was greater than in an abluminal cell (pericyte) located on a capillary. Thus, although our electrophysiological experiments could not exclude that the greater VDCC current detected in the feeder vessels simply reflected their having a higher density of abluminal cells, the monitoring VDCC-dependent calcium changes in individual abluminal cells revealed that VDCC function is greater in mural cells of the feeder vessel than in pericytes of the capillaries.

To further assess the role of VDCCs in the functioning of the retinal microvasculature, we used time-lapse photography to detect VDCC-dependent changes in the contractile tone of abluminal cells (Figs. 8A, 8B; Movie S1, http://www.iovs.org/cgi/content/full/51/11/5979/DC1). We observed that during exposure of retinal microvessels to 97.5 mM $K^+$ (solution D), 65% ($n = 66$) of the feeder vessel mural cells contracted (Fig. 8A). Furthermore, this depolarization-induced contraction was blocked by nifedipine (Fig. 8A). In contrast to the depolarization-induced contraction of feeder vessel mural cells, only 1 of 157 monitored capillary pericytes contracted during exposure to the depolarizing perfusate; this was a significantly ($P < 0.0001$, Fisher exact test) smaller response rate. These observations support an operational model of the feeder vessel/capillary unit in which VDCC-driven contraction occurs almost exclusively in the feeder vessels.

To further evaluate the functional implications of VDCC function being markedly greater in feeder vessels than in capillaries, we quantified the effect of a 97.5 mM $K^+$ on lumen diameter. As shown in Figure 8C, depolarization induced by 97.5 mM $K^+$ caused the lumens of the feeder vessels to narrow by 28% ± 6%; this significant change ($P < 0.0001$; $n = 5$) was mediated by a nifedipine-sensitive mechanism (Fig. 8C). In contrast to the depolarization-induced constriction of feeder vessels, the lumen diameters of the capillaries were not significantly ($P = 0.4$) altered during exposure to 97.5 mM $K^+$ (Fig. 8D). Based on these observations using time-lapse photography, we concluded that VDCC-driven vasomotor responses occurred chiefly in the feeder vessel portion of the feeder vessel/capillary unit.

To complement observations on the effect of depolarization, we also assessed the effect of hyperpolarization on the contractile tone of abluminal cells. We observed that a perfusate containing 10 mM $K^+$ (solution C) caused 29% of the feeder vessel mural cells to relax; nifedipine significantly ($P < 0.0001$, Fisher exact test) blocked this response. In contrast ($P < 0.0001$, Fisher exact test), only 2% of the capillary pericytes relaxed during exposure to solution C. In other experiments, we used pinacidil as a pharmacologic tool to activate hyperpolarizing $K_{ATP}$ channels, which are predominately located in the capillaries of the retinal microvasculature.[5] As summarized in Figure 9, 30% of the mural cells located on the feeder vessels relaxed through a nifedipine-sensitive ($P < 0.0001$, Fisher exact test) mechanism during exposure to pinacidil. In contrast ($P < 0.0001$, Fisher exact test), pericyte relaxation was not observed in response to this $K_{ATP}$ activator. These findings provide further evidence that VDCC-driven vasomotor responses occur chiefly in the feeder vessels even when the voltage change is generated in the capillaries.

We postulated that the pinacidil-induced relaxation of feeder vessel mural cells is dependent on gap junctions to transmit the hyperpolarization generated by capillary $K_{ATP}$ channels. To garner evidence for this scenario, we quantified pinacidil-induced relaxation in microvessels treated with GAP 27, a peptide that inhibits gap junction transmission in the retinal microvasculature.[17] As shown in Figure 9, after GAP 27

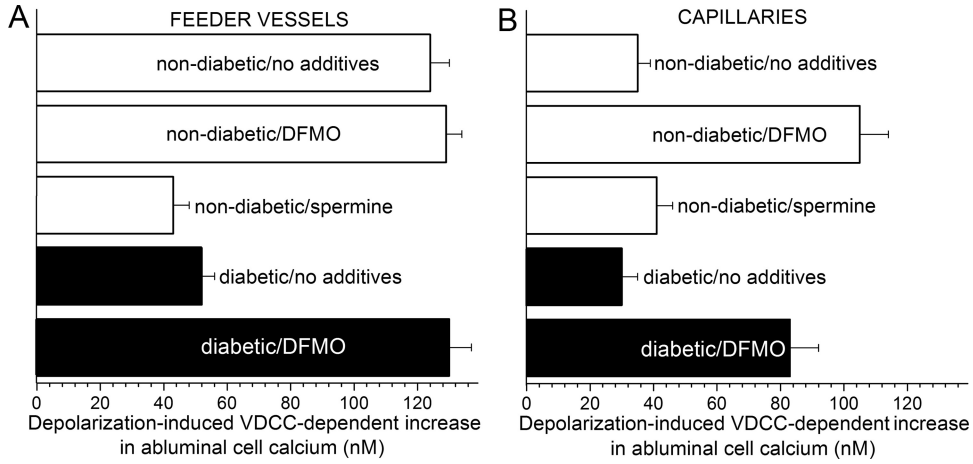


**FIGURE 7.** Depolarization-induced VDCC-dependent increases in abluminal cell calcium in retinal feeder vessels and capillaries. VDCC function was assessed by determining the maximum nifedipine-sensitive change in intracellular calcium during exposure to solution D (97.5 mM $K^+$). (**A**) VDCC-dependent increase in the intracellular calcium concentration of abluminal cells located on feeder vessels in nondiabetic (*white bars*) and diabetic (*black bars*) microvascular complexes. The number of monitored feeder vessel mural cells was 180, 71, 32, 79, and 52 for the nondiabetic/no additives group, the nondiabetic/DFMO group, the nondiabetic/spermine group, the diabetic/no additives group, and the diabetic/DFMO group, respectively. For each group, 23 ± 3 mural cells were monitored in the nifedipine-containing solutions. (**B**) VDCC-dependent increase in pericyte calcium in nondiabetic (*white bars*) and diabetic (*black bars*) capillaries. For the nondiabetic/no additives group, the nondiabetic/DFMO group, the nondiabetic/spermine group, the diabetic/no additives group, and the diabetic/DFMO group, 62, 61, 22, 27, and 30 capillary pericytes were monitored, respectively. For each group, 18 ± 4 pericytes were monitored in the nifedipine-containing solutions.

treatment, pinacidil caused only 4% of the feeder vessel mural cells to relax; this was significantly ($P < 0.0001$, Fisher exact test) less than the 30% response rate observed in control microvessels. Based on these experiments, we concluded that a vasomotor response triggered by the activation of $K_{ATP}$ channels in the capillary network requires that the hyperpolarization be transmitted through gap junction pathways to the VDCC-rich feeder vessels.

## Regulation of Microvascular VDCC Function by Spermine

What accounts for the topographical variation in VDCC function within the feeder vessel/capillary unit? Clearly, there are many possible mechanisms. Here, we focused on the possible role of endogenous spermine, which was of interest because this polyamine is known to inhibit L-type VDCCs in various tissues[9–11] and has been shown to regulate the function of various ion channels in retinal capillaries.[5,8] To assess whether endogenous spermine may regulate VDCC function in the feeder vessel/capillary unit, we preincubated microvascular complexes in solution A supplemented with DFMO, whose inhibition of ornithine decarboxylase blocked polyamine synthesis. Of note, we found that DFMO did not significantly alter the resting membrane potential of retinal microvessels ($n = 5$).

As summarized in Figure 7B, DFMO treatment markedly ($P < 0.0001$) enhanced the VDCC-dependent increase in pericyte calcium observed during exposure to the depolarizing perfusate, solution D (97.5 mM $K^+$). In contrast, the 97.5 mM $K^+$-induced increase in the calcium concentration of feeder vessel mural cells was not significantly affected by DFMO (Fig. 7A), and the increase induced by 97.5 mM $K^+$ remained robust. Because of the boost in capillary VDCC function, DFMO treatment of retinal microvessels resulted in feeder vessels and capillaries with similar depolarization-induced, VDCC-dependent increases in abluminal cell calcium. Based on these results, we concluded that endogenous spermine suppresses VDCC function in the pericytes of retinal capillaries.

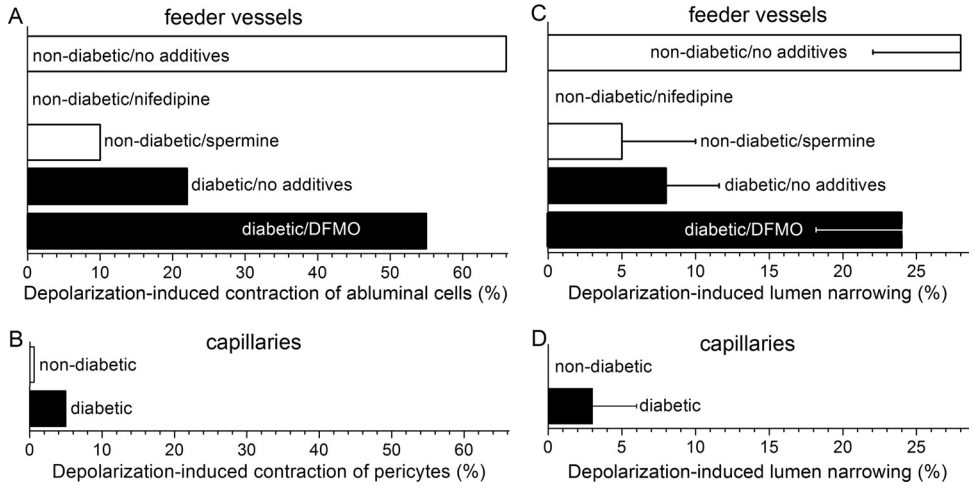


**FIGURE 8.** Abluminal cell contraction and lumen narrowing during exposure of diabetic and nondiabetic microvessels to 97.5 mM $K^+$. (**A**) Percentage of feeder vessel mural cells contracting during solution D-induced depolarization. In the nondiabetic/no additives, nondiabetic/nifedipine, nondiabetic/spermine, diabetic/no additives, and diabetic/DFMO groups, the number of monitored mural cells was 45, 45, 21, 41, and 38, respectively. (**B**) Percentage of capillary pericytes that contracted when exposed to solution D. The number of monitored pericytes for the nondiabetic and the diabetic groups was 157 and 40, respectively; the response rate for the nondiabetic and diabetic groups was not significantly different ($P = 1.0$, Fisher exact test). (**C**) 97.5 mM $K^+$-induced narrowing of the lumen of feeder vessels. Measurements were made in the same sets of microvessels as in (**A**). The lumen diameter before exposure to solution D was 3.4 ± 0.2 μm ($n = 24$ feeder vessels). For the nondiabetic/no additives, nondiabetic/nifedipine, nondiabetic/spermine, diabetic/no additives, and diabetic/DFMO groups, the number of monitored microvessels was 5, 5, 5, 5, and 4, respectively. (**D**) 97.3 mM $K^+$-induced lumen narrowing in capillaries of nondiabetic ($n = 12$) and diabetic ($n = 8$) microvascular complexes; lumen constriction of nondiabetic and diabetic capillaries was not significantly different ($P = 0.4$). Before exposure to solution D, the capillary lumen diameter was 3.3 ± 0.2 μm ($n = 20$ capillaries). Measurements were made in the same sets of microvessels as in (**B**).

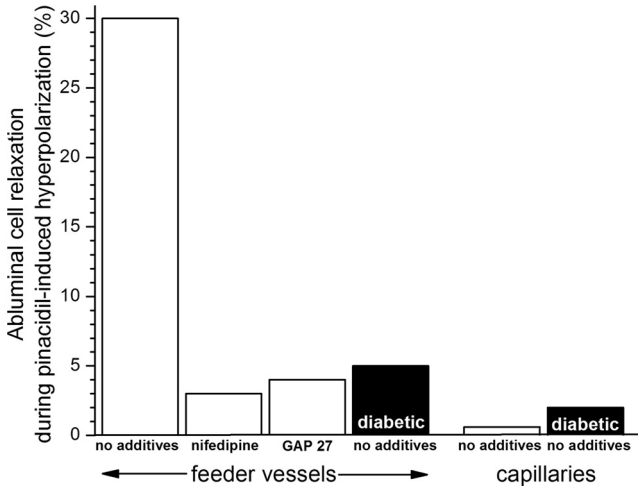


**FIGURE 9.** Percentage of monitored abluminal cells that relaxed during hyperpolarization induced by 5 $\mu$M pinacidil, an activator of microvascular $K_{ATP}$ channels.[5,38] For the nifedipine-containing group, microvessels were pre-exposed to solution A supplemented with 10 $\mu$M nifedipine for 10 to 15 minutes. For the GAP 27 group, microvessels were pre-exposed to solution A supplemented with 300 $\mu$M GAP 27 for 2 hours; 60- to 90-minute exposure to this concentration of GAP 27 eliminated gap junction transmission in retinal microvessels.[17] For feeder vessels, the number of monitored abluminal (mural) cells was 66, 29, 53, and 166 for the no additives, nifedipine, GAP 27, and diabetic/no additives group, respectively. For capillaries, the number of monitored abluminal cells (pericytes) was 25 and 49 for the no additives and the diabetic/no additives group, respectively.

## Diabetic Alteration of Microvascular VDCC Function

We asked whether diabetes, which is known to alter the function of $K_{IR}$ and $K_{ATP}$ channels in retinal feeder vessels,[5,8] also affects the function of microvascular VDCCs. To help determine whether VDCC function is changed in diabetic microvessels, VDCC currents were recorded in retinal microvascular complexes isolated from rats made diabetic by streptozotocin. As shown in Figures 10A, 10B, and 10E, the density of the VDCC current detected in perforated-patch recordings from diabetic feeder vessels was significantly ($P = 0.0136$) smaller than the VDCC current density in nondiabetic feeder vessels. Given that diabetes did not significantly alter the membrane capacitance (see Methods), this decrease reflected a decrease in VDCC current generated in the feeder vessels. In contrast to diabetes having an effect on VDCCs in the feeder vessels, we found that diabetes did not significantly affect the density of the VDCC current in retinal capillaries (Figs. 10C–E); the membrane capacitance was also unaffected by diabetes.

To provide additional evidence that diabetes decreases VDCC function in the feeder vessels, calcium-imaging experiments were performed. Figure 7A summarizes these experiments. We observed that in comparison with nondiabetic feeder vessels, exposure of diabetic feeder vessels to 97.5 mM $K^+$ (solution D) induced a significantly ($P < 0.0001$) smaller VDCC-dependent increase in mural cell calcium. In contrast, diabetes did not significantly ($P = 0.6$) affect the depolarization-induced VDCC-dependent increase in pericyte calcium; VDCC function in capillary pericytes remained very low (Fig. 7B). Thus, the results of these calcium-imaging experiments were consistent with our electrophysiological study findings indicating that diabetes diminishes VDCC function in the feeder vessels of the retinal microvasculature.

To help determine the effect of diabetes on VDCC-driven vasomotor responses, we assessed how diabetes affected the VDCC-dependent contractile responses of the abluminal cells. In one set of experiments, pinacidil was used to activate a hyperpolarizing $K_{ATP}$ current. In these experiments, the percentage of feeder vessel mural cells that relaxed in response to the pinacidil-induced hyperpolarization was markedly ($P < 0.0001$, Fisher exact test) lower in feeder vessels of the diabetic, compared with the nondiabetic, retina (Fig. 9). Of note, this diminution occurred even though this $K_{ATP}$ activator induced a larger hyperpolarization in diabetic microvessels.[5] In contrast to the effect of diabetes on feeder vessel VDCCs, the ability of pinacidil to cause capillary pericytes to relax was not significantly altered by diabetes; the response rate of pericytes remained minimal (Fig. 9).

The effect of diabetes on the depolarization-induced contraction of abluminal cells was also assessed. As summarized in Figure 8A, diabetes diminished the contractile response of feeder vessel mural cells to depolarization induced by 97.5 mM $K^+$. Only 22% of the mural cells on diabetic feeder vessels were observed to contract; this was significantly ($P < 0.0001$, Fisher exact test) lower than the 65% response rate in nondiabetic feeder vessels.

Indicative of the functional significance of the diabetes-induced inhibition of feeder vessel VDCCs, depolarization caused by exposure to 97.5 mM $K^+$ resulted in significantly ($P = 0.0128$) less narrowing of the lumens of diabetic feeder vessels (Fig. 8C). Specifically, there was only a 5% ± 5% constriction of the lumens of diabetic feeder vessels during exposure to the high $K^+$ solution. This contrasted ($P = 0.0117$) with the 28% ± 5% narrowing induced in nondiabetic feeder vessels exposed to 97.5 mM $K^+$. In the case of diabetic capillaries, lumen narrowing during exposure to 97.5 mM $K^+$ remained minimal and was not significantly different from that of nondiabetic capillaries (Fig. 8D).

## Action of Spermine in Diabetic Microvessels

By what mechanism does diabetes cause the inhibition of feeder vessel VDCCs? Because spermine is increased in the diabetic eye[27] and plays an enhanced role in the precapillary feeder vessels of the diabetic retina,[5,8] we postulated that endogenous spermine may play a role in the diabetes-induced inhibition of feeder vessel VDCCs. To help test this hypothesis, diabetic microvessels were exposed to the inhibitor of polyamine synthesis, DFMO. We found that DFMO significantly ($P < 0.0001$) reversed the attenuating effect of diabetes on the depolarization-induced increase in the calcium concentration of feeder vessel mural cells (Fig. 7A). In addition, DFMO reversed ($P = 0.0028$) the inhibitory effect of diabetes on the 97.5 mM $K^+$-induced contraction of feeder vessel mural cells (Fig. 8A). Furthermore, DFMO significantly ($P = 0.0474$) reversed the attenuating effect of diabetes on the ability of feeder vessels to constrict during exposure to this depolarizing perfusate (Fig. 8C).

Additional evidence that spermine may play a role in mediating the diabetes-induced inhibition of feeder vessel VDCCs was provided by experiments showing that the effects of diabetes could be mimicked by exposing nondiabetic microvessels to this polyamine. As summarized in Figure 7A, preincubation of nondiabetic microvessels in solution A supplemented with 5 mM spermine significantly diminished ($P < 0.0001$) the 97.5 mM $K^+$-induced increase in the calcium concentration of feeder vessel mural cells. Consistent with the ability of spermine to inhibit microvascular VDCCs, exposure to this polyamine significantly ($P < 0.0001$) decreased the basal concentration of calcium in the mural cells of nondiabetic feeder vessels through a nifedipine-sensitive mechanism (Fig. 11). Of note, this spermine-mediated decrease in basal VDCC activity occurred despite the 9 mV depolarization caused by spermine inhibition of the outward $K_{IR}$ cur-

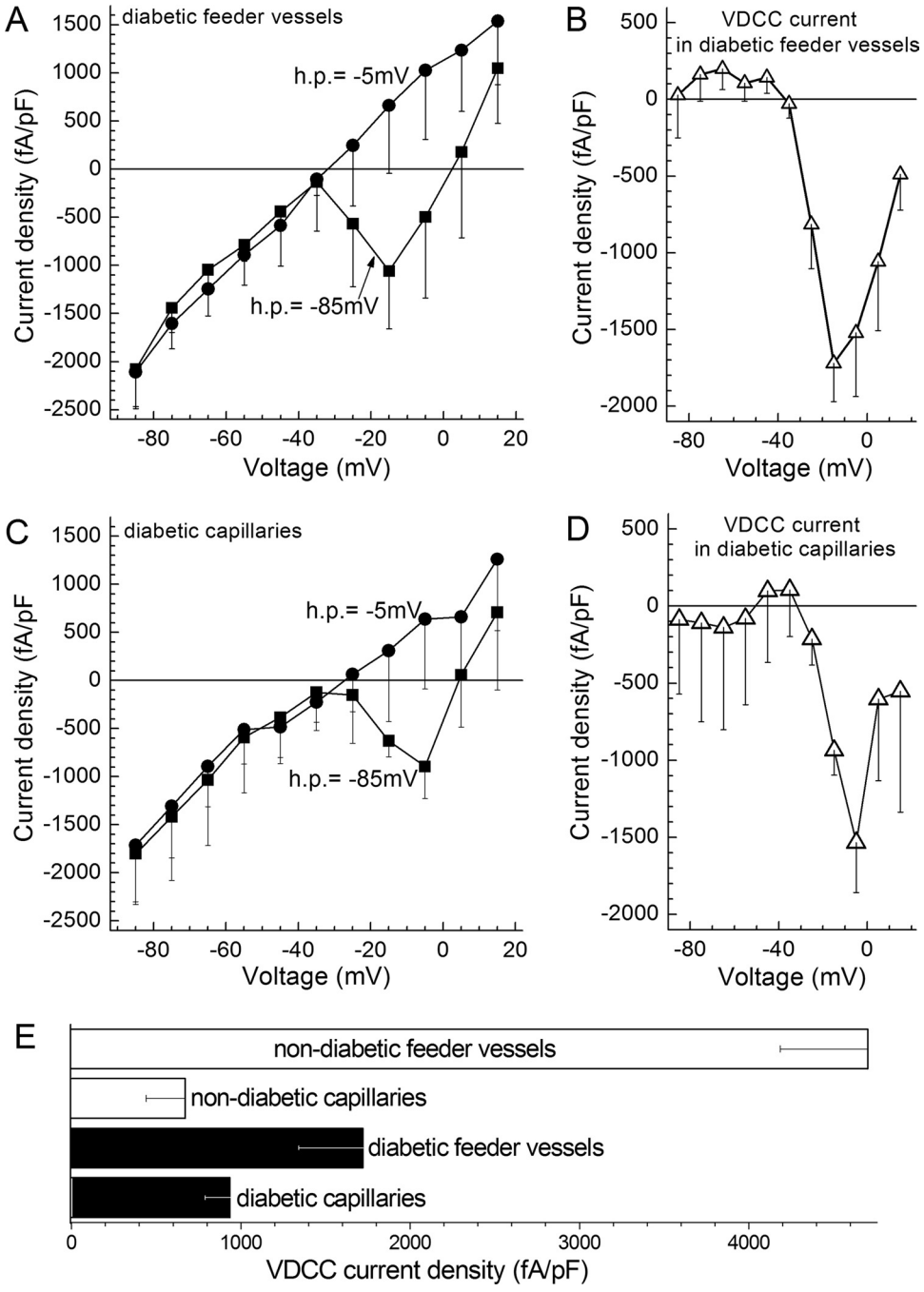


**FIGURE 10.** VDCC currents in feeder vessels and capillaries of the diabetic retina. (**A**) Plots of the peak inward current density versus test potential recorded from mural cells ($n = 6$) located on feeder vessels in retinal microvascular complexes from rats made diabetic by streptozotocin. Currents were generated from a holding potential of −85 mV (*squares*) or −5 mV (*circles*). (**B**) The difference of the plots in (**A**). (**C**) Plots of the peak inward current density versus test potential recorded from pericytes ($n = 4$) located on capillaries within diabetic microvascular complexes. Currents were generated from a holding potential of −85 mV (*squares*) or −5 mV (*circles*). (**D**) The difference of the plots in (**C**). (**E**) Maximum inward VDCC current densities recorded from abluminal cells of feeder vessels and capillaries in nondiabetic and diabetic retinal microvascular complexes. Data for the nondiabetic groups are from Figures 3C and 3G.

rent in retinal microvessels.[8] In other experiments, we found that similar to the effect of diabetes, pre-exposure of nondiabetic microvessels to spermine significantly ($P < 0.0001$, Fisher exact test) diminished the 97.5 mM $K^+$-induced contraction of feeder vessel mural cells (Fig. 7A). We also observed that the attenuating effect of diabetes on the depolarization-induced narrowing of the feeder vessel lumens (Fig. 8C) could be mimicked by exposing nondiabetic microvessels to spermine (Fig. 8C); this polyamine significantly ($P = 0.0398$) diminished the 97.5 mM $K^+$-induced constriction of the lumens of the feeder vessels.

## DISCUSSION

As reviewed in Figure 12, this study of microvascular complexes freshly isolated from the rat retina showed that VDCC-mediated changes in ionic currents, intracellular calcium, abluminal cell contractility, and lumen diameter are markedly greater in the precapillary feeder vessels than in the capillaries. We found that this difference in VDCC function is, in large part, due to the inhibition of capillary VDCCs by endogenous spermine, a polyamine known to inhibit L-type calcium channels.[9–13] Our experiments also revealed that early in the course of diabetes, VDCC function in the feeder vessels becomes inhibited by a spermine-dependent mechanism. In addition, we demonstrated that as an operational consequence of the diabetes-induced inhibition feeder vessel VDCCs, the ability of the feeder vessel/capillary unit to generate voltage-driven vasomotor responses becomes markedly compromised in the diabetic microvasculature. Based on this study, we concluded that in both the normal and the diabetic retina, spermine plays

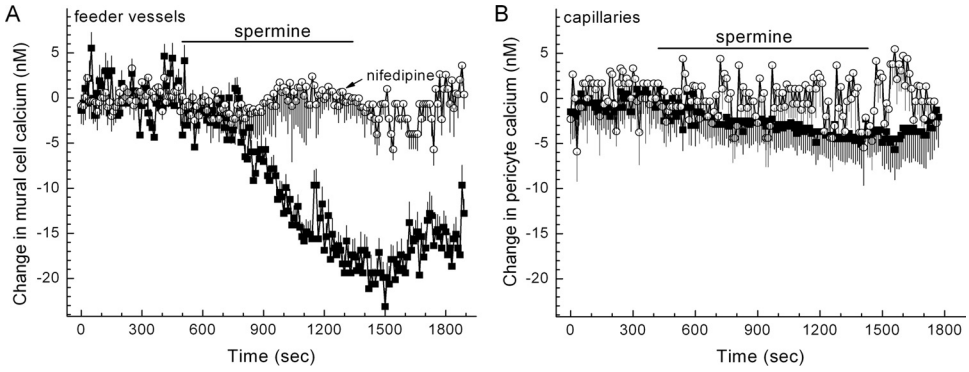


**FIGURE 11.** Effect of spermine on abluminal cell calcium. (**A**) Plot of the mean change in intracellular calcium versus time for abluminal cells located on feeder vessels. The *bar* indicates when the perfusate (solution A) was supplemented with 5 mM spermine without (*squares*) or with (*circles*) 10 $\mu$M nifedipine. The number of abluminal cells monitored was 31 and 16 for the nifedipine-free and the nifedipine-containing group, respectively. (**B**) Plot of the mean change in pericyte calcium versus time. The *bar* indicates when the perfusate (solution A) was supplemented with 5 mM spermine without (*squares*) or with (*circles*) 10 $\mu$M nifedipine. The number of monitored pericytes was 27 and 11 for the nifedipine-free and the nifedipine-containing group, respectively.

a critical role in the regulation of VDCC function at the most decentralized site for the regulation of retinal blood flow (i.e., the feeder vessel/capillary unit).

Our finding that functional VDCCs are chiefly located in the precapillary feeder vessels supports the emerging concept of operational specialization within the feeder vessel/capillary unit. This finding also provides additional evidence that the regulation of ion channel function by endogenous spermine accounts for important operational differences between feeder vessels and capillaries. For example, previously we reported that endogenous spermine enhances $K_{ATP}$ channel function in the capillaries and, as a consequence, that this portion of the feeder vessel/capillary unit generates almost all the hyperpolarizing $K_{ATP}$ current activated by the vasoactive signal adenosine.[8] In addition, we recently found that the increase in membrane resistance associated with spermine's inhibition of capillary $K_{IR}$ channels enhanced the voltage changes induced by vasoactive signals.[8] However, though the spermine-mediated effects on $K_{IR}$ and $K_{ATP}$ channels helped make retinal capillaries well adapted for generating voltages in response to extracellular signals, the study presented here revealed that the inhibition of capillary VDCCs by endogenous spermine limits the ability of capillaries to transduce a change in voltage into a vasomotor response. On the other hand, the abundance of functional VDCCs in the feeder vessels makes them well equipped to convert a voltage transmitted from the capillaries into a change in mural cell calcium and, thereby, an alteration in mural cell contractility, lumen diameter, and blood flow. Based on our studies of the functional organization of the feeder vessel/capillary unit, we conclude that the spermine-mediated regulation of ion channels enhances the ability of capillaries to generate voltage changes in response to vasoactive signals but attenuates their capability to instigate VDCC-driven vasomotor responses.

Although VDCC function is minimal in retinal capillaries, it is important to note that evidence is accumulating that retinal blood flow can be regulated at the capillary level by non–VDCC-dependent mechanisms. In support of this concept, numerous extracellular molecules trigger a change in pericyte calcium, pericyte contractility, and capillary lumen diameter.[3,4,17,20,28,29] However, we have reported that VDCCs have only a modulatory role.[21] Rather, vasoactive signals induce localized capillary constrictions or dilations by way of VDCC-independent mechanisms involving the activation of calcium-permeable, nonspecific cation channels, the release of calcium stores, or the action of the sodium/calcium exchanger.[17,19,21] However, because of efficient gap junction-mediated transmission in the retinal microvasculature,[6] a voltage change generated in the capillary network can result in a voltage-driven vasomotor responses in the VDCC-rich feeder vessel.

In this first assessment of the effect of diabetes on the function of VDCCs in the feeder vessel/capillary unit, we ob-

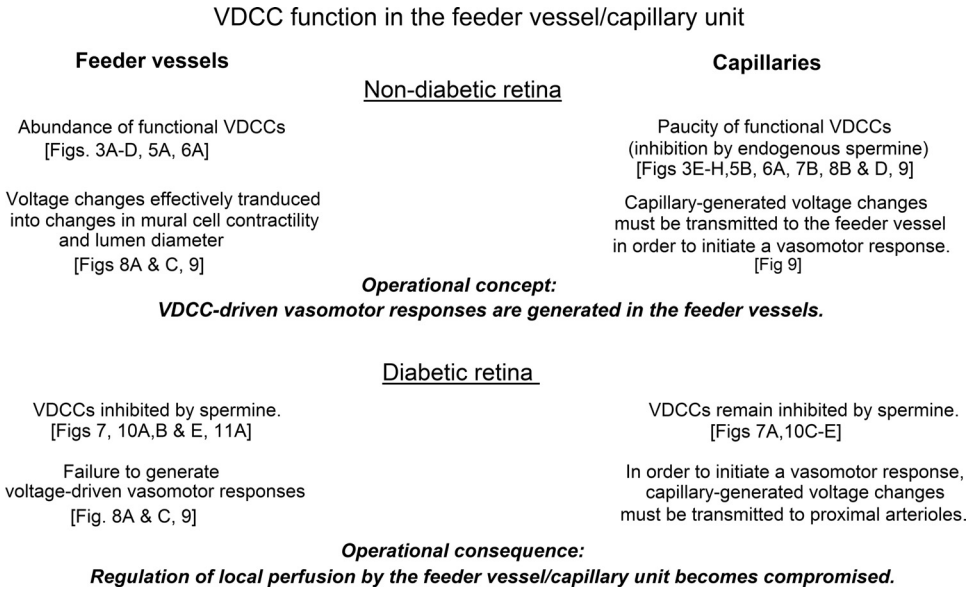


**FIGURE 12.** Overview of experimental findings and conclusions concerning VDCC function in the feeder vessel/capillary unit of the normal and the diabetic retina.

served that voltage-driven changes in the lumen diameters of the feeder vessels are markedly diminished because of the spermine-dependent inhibition of VDCCs. Most likely, the diabetes-induced inhibition of feeder vessel VDCCs compromises the ability of the feeder vessel/capillary unit to serve effectively as the most decentralized site for the regulation of retinal perfusion. Perhaps as a consequence of this dysfunction, diabetic retinopathy may progress.

Although no previous studies have determined the effect of diabetes on the function of L-type VDCCs in the retinal microvasculature, diabetes is known to alter the activity of these channels in nonretinal vascular beds and in nonvascular tissues. Paradoxically, the effects of diabetes on VDCC function in the circulatory system are variable. On the one hand, arteriolar L-type VDCC activity is attenuated in the kidney[30] and tail[31] of diabetic rats. On the other hand, VDCC activity appears to be increased in mesenteric,[32] skeletal,[33] and cerebral[34] arteriolar myocytes. Although the mechanistic basis for the variable effects of diabetes on vascular VDCCs is unclear, this variability requires that investigators determine the effect of diabetes for each vascular bed. For the feeder vessel/capillary unit of the retinal vasculature, our study establishes that VDCC function in the feeder vessels becomes attenuated soon after the onset of diabetes.

Our finding that VDCC function is inhibited in the distal microvasculature of the diabetic retina is without precedent, though investigators have studied the effect of diabetes at more proximal locations and have assessed the effect of hyperglycemia on retinal pericytes in culture. For example, McGinty et al.[35] found decreased VDCC activity in pericytes cultured in 25 mM glucose. However, perhaps because hyperglycemia in vitro does not fully mimic diabetes, our study of microvascular complexes did not reveal a significant effect of diabetes on VDCC function in the pericyte-containing capillaries. Rather, we found that in the diabetic microvasculature, VDCC activity remained very low in the capillary network and that VDCC function in the feeder vessels was markedly diminished. Interestingly, in contrast to our finding that diabetes inhibits VDCC function in feeder vessels whose diameters are $<10$ $\mu$m, a study of retinal arterioles with diameters $>30$ $\mu$m found that the VDCC current was not altered after 3 months of streptozotocin-induced diabetes.[36] These observations led us to postulate that VDCC function in the feeder vessel portion of the retinal vasculature is particularly vulnerable to diabetes.

In this study, our ability to isolate vast complexes of the retinal microvasculature allowed the use of the patch-clamp technique, calcium imaging, and time-lapse photography to detect VDCC-dependent changes in the ionic currents, intracellular calcium, abluminal cell contractility, and lumen diameter in feeder vessels and capillaries. Furthermore, the ability to physically separate capillaries from the proximal portion of an isolated microvascular complex permitted detection of ionic currents generated exclusively within the capillary network. An additional advantage of studying isolated microvessels is that the effects of chemicals, such as spermine and DFMO, could be assessed in the absence of potentially confounding responses of nonvascular cells. However, because we did not internally perfuse the isolated microvessels, the effect of blood flow on VDCC function was not evaluated. In addition, it remains to be determined whether the spermine-mediated inhibition of microvascular VDCCs involves an allosteric modulation of the dihydropyridine binding site, as proposed for spermine's regulation of VDCCs in nonretinal CNS cells.[10] Further studies are needed to assess whether the spermine-mediated effects of diabetes on the function of VDCCs in the precapillary feeder vessels involve the activity of arginase, whose upregulation in diabetic blood vessels[37] boosts the production of ornithine, which is a polyamine precursor. Of course, it will also be necessary to verify that conclusions derived from studies of isolated microvessels apply in vivo, even though this will require technical advances to permit the assessment of VDCC function in the feeder vessel/capillary unit of the retina in vivo. An additional caveat is that extrapolation of this study's findings to other vascular beds is risky because the circulatory system of the retina is specially adapted to meet the unique challenge of supplying oxygen and nutrients to a translucent tissue.

In conclusion, this study revealed topographical heterogeneity in the distribution of functional VDCCs within the feeder vessel/capillary unit of the retina—namely, VDCC function is greater in feeder vessels than in capillaries. In large part, this difference is due to the inhibition of capillary VDCCs by spermine. Our experiments showed that as a consequence of capillary VDCCs being inhibited by this polyamine, a capillary-generated voltage change must be transmitted to the feeder vessel whose VDCCs generate changes in mural cell calcium, abluminal cell contractility, and lumen diameter. In addition, our results show that through a spermine-dependent mechanism, diabetes causes VDCC inhibition in the precapillary feeder vessels and may thereby compromise the ability of the feeder vessel/capillary unit to function as the most decentralized site for the regulation of retinal blood flow (Fig. 12).

## *Acknowledgments*

The authors thank Bret Hughes for helpful discussions and for use of equipment.

## *References*

1. Funk RH. Blood supply of the retina. *Ophthalmic Res.* 1997;29:320–325.
2. Shepro D, Morel NM. Pericyte physiology. *FASEB J.* 1993;7:1031–1038.
3. Peppiatt CM, Howarth C, Mobbs P, Attwell D. Bidirectional control of CNS capillary diameter by pericytes. *Nature.* 2006;443:700–704.
4. Puro DG. Physiology and pathobiology of the pericyte-containing retinal microvasculature: new developments. *Microcirculation.* 2007;14:1–10.
5. Ishizaki E, Fukumoto M, Puro DG. Functional $K_{ATP}$ channels in the rat retinal microvasculature: topographical distribution, redox regulation, spermine modulation and diabetic alteration. *J Physiol.* 2009;587:2233–2253.
6. Wu DM, Miniami M, Kawamura H, Puro DG. Electrotonic transmission within pericyte-containing retinal microvessels. *Microcirculation.* 2006;13:353–363.
7. Oku H, Kodama T, Sakagami K, Puro DG. Diabetes-induced disruption of gap junction pathways within the retinal microvasculature. *Invest Ophthalmol Vis Sci.* 2001;42:1915–1920.
8. Matsushita K, Puro DG. Topographical heterogeneity of $K_{IR}$ currents in pericyte-containing microvessels of the rat retina: effect of diabetes. *J Physiol.* 2006;573:483–495.
9. Gomez M, Hellstrand P. Effects of polyamines on voltage-activated calcium channels in guinea-pig intestinal smooth muscle. *Pflugers Arch.* 1995;430:501–507.
10. Schoemaker H. Polyamines allosterically modulate [$^3$H]nitrendipine binding to the voltage-sensitive calcium channel in rat brain. *Eur J Pharmacol.* 1992;225:167–169.
11. Scott RH, Sutton KG, Dolphin AC. Interactions of polyamines with neuronal ion channels. *Trends Neurosci.* 1993;16:153–160.
12. Cayzac S, Rocher A, Obeso A, Gonzalez C, Kemp PJ, Riccardi D. Effects of the polyamine spermine on arterial chemoreception. *Adv Exp Med Biol.* 2009;648:97–104.
13. Gomez M, Hellstrand P. Endogenous polyamines modulate $Ca^{2+}$ channel activity in guinea-pig intestinal smooth muscle. *Pflugers Arch.* 1999;438:445–451.
14. Zhao HB, Santos-Sacchi J. Effect of membrane tension on gap junctional conductance of supporting cells in Corti's organ. *J Gen Physiol.* 1998;112:447–455.

15. Sakagami K, Wu DM, Puro DG. Physiology of rat retinal pericytes: modulation of ion channel activity by serum-derived molecules. *J Physiol.* 1999;521:637–650.
16. Bean BP. Classes of calcium channels in vertebrate cells. *Annu Rev Physiol.* 1989;51:367–384.
17. Yamanishi S, Katsumura K, Kobayashi T, Puro DG. Extracellular lactate as a dynamic vasoactive signal in the rat retinal microvasculature. *Am J Physiol.* 2006;290:H925–H934.
18. Grynkiewicz G, Poenie M, Tsien RY. A new generation of $Ca^{2+}$ indicators with greatly improved fluorescence properties. *J Biol Chem.* 1985;260:3440–3450.
19. Kawamura H, Sugiyama T, Wu DM, et al. ATP: a vasoactive signal in the pericyte-containing microvasculature of the rat retina. *J Physiol.* 2003;551:787–799.
20. Wu DM, Kawamura H, Sakagami K, Kobayashi M, Puro DG. Cholinergic regulation of pericyte-containing retinal microvessels. *Am J Physiol.* 2003;284:H2083–H2090.
21. Kawamura H, Kobayashi M, Li Q, et al. Effects of angiotensin II on the pericyte-containing microvasculature of the rat retina. *J Physiol.* 2004;561:671–683.
22. Hell JW, Westenbroek RE, Warner C, et al. Identification and differential subcellular localization of the neuronal class C and class D L-type calcium channel alpha 1 subunits. *J Cell Biol.* 1993;123:949–962.
23. Edwards FR, Hirst GD, Silverberg GD. Inward rectification in rat cerebral arterioles; involvement of potassium ions in autoregulation. *J Physiol.* 1988;404:455–466.
24. Quayle JM, Dart C, Standen NB. The properties and distribution of inward rectifier potassium currents in pig coronary arterial smooth muscle. *J Physiol.* 1996;494(pt 3):715–726.
25. Chrissobolis S, Sobey CG. Inwardly rectifying potassium channels in the regulation of vascular tone. *Curr Drug Targets.* 2003;4:281–289.
26. Curtis TM, Scholfield CN. Nifedipine blocks $Ca^{2+}$ store refilling through a pathway not involving L-type $Ca^{2+}$ channels in rabbit arteriolar smooth muscle. *J Physiol.* 2001;532:609–623.
27. Li Q, Puro DG. Adenosine activates ATP-sensitive $K^+$ currents in pericytes of rat retinal microvessels: role of $A_1$ and $A_{2a}$ receptors. *Brain Res.* 2001;907:93–99.
28. Nicoletti R, Venza I, Ceci G, Visalli M, Teti D, Reibaldi A. Vitreous polyamines spermidine, putrescine, and spermine in human proliferative disorders of the retina. *Br J Ophthalmol.* 2003;87:1038–1042.
29. Sakagami K, Kodama T, Puro DG. PDGF-induced coupling of function with metabolism in microvascular pericytes of the retina. *Invest Ophthalmol Vis Sci.* 2001;42:1939–1944.
30. Schonfelder U, Hofer A, Paul M, Funk RH. In situ observation of living pericytes in rat retinal capillaries. *Microvasc Res.* 1998;56:22–29.
31. Carmines PK, Ohishi K, Ikenaga H. Functional impairment of renal afferent arteriolar voltage-gated calcium channels in rats with diabetes mellitus. *J Clin Invest.* 1996;98:2564–2571.
32. Wang Z, Haydon PG, Yeung ES. Direct observation of calcium-independent intercellular ATP signaling in astrocytes. *Anal Chem.* 2000;72:2001–2007.
33. White RE, Carrier GO. Vascular contraction induced by activation of membrane calcium ion channels is enhanced in streptozotocin-diabetes. *J Pharmacol Exp Ther.* 1990;253:1057–1062.
34. Ungvari Z, Pacher P, Kecskemeti V, Papp G, Szollar L, Koller A. Increased myogenic tone in skeletal muscle arterioles of diabetic rats: possible role of increased activity of smooth muscle $Ca^{2+}$ channels and protein kinase C. *Cardiovasc Res.* 1999;43:1018–1028.
35. Navedo MF, Takeda Y, Nieves-Cintron M, Molkentin JD, Santana LF. Elevated $Ca^{2+}$ sparklet activity during acute hyperglycemia and diabetes in cerebral arterial smooth muscle cells. *Am J Physiol Cell Physiol.* 2010;298:C211–C220.
36. McGinty A, Scholfield CN, Liu WH, Anderson P, Hoey DE, Trimble ER. Effect of glucose on endothelin-1-induced calcium transients in cultured bovine retinal pericytes. *J Biol Chem.* 1999;274:25250–25253.
37. McGahon MK, Zhang X, Scholfield CN, Curtis TM, McGeown JG. Selective downregulation of the BK$\beta$1 subunit in diabetic arteriolar myocytes. *Channels (Austin).* 2007;1:141–143.
38. Romero MJ, Platt DH, Tawfik HE, et al. Diabetes-induced coronary vascular dysfunction involves increased arginase activity. *Circ Res.* 2008;102:95–102.